

Modeling the circulation in the Gulf of Tonkin, South China Sea

Jingsong Gao · Huijie Xue · Fei Chai · Maochong Shi

Received: 29 August 2012 / Accepted: 28 May 2013 / Published online: 6 July 2013
© Springer-Verlag Berlin Heidelberg 2013

Abstract The circulation in the Gulf of Tonkin (Beibu Gulf) was studied using the Princeton Ocean Model, which was forced with the daily surface and lateral boundary fluxes for 2006 and 2007, as well as tidal harmonics and monthly climatological river discharges. In the southern Gulf, the vertically averaged circulation was anti-cyclonic in summer and changed to cyclonic in winter. Although it was highly correlated with the local wind, the southern gyre was driven primarily by the South China Sea (SCS) general circulation from the south. Flows in the Qiongzhou Strait that played a significant role in determining the circulation variability in the northeastern Gulf could be eastward or westward at any given day in summer or winter, but the seasonal mean current was eastward from late spring through summer and westward during the rest of the year, with an annual mean westward transport of ~ 0.1 Sv into the Gulf. Different water masses were distinguished at the surface with the warm and saline SCS water in the south, relatively fresh plume waters along the northern and western coasts of the Gulf, and the mixture of the two in between. At lower levels, two cold water masses were identified in the model, and each had T/S distributions qualitatively similar to the observations obtained in 2007. These two water masses were produced

throughout the winter, sheltered from the surface warming by a thermocline as the season progressed, and eventually disappeared in late fall.

Keywords Gulf of Tonkin · Qiongzhou Strait · Circulation · Water masses

1 Introduction

The Gulf of Tonkin (also called the Beibu Gulf; “Gulf”, hereinafter) is located in the northwestern South China Sea (SCS), from $\sim 17^\circ\text{N}$ to 22°N and from $\sim 105^\circ\text{E}$ to 110°E (Fig. 1). The Gulf is a shallow coastal water body with the water depth less than 100 m, and it is rich with oil and fishery resources. In the past decades, the circulation in the Gulf has been deduced often as a byproduct of studies about the SCS. Dale (1956) first pointed out that the surface circulation in the SCS was driven by the monsoon wind. Wyrтки (1961) analyzed the seasonal surface circulation patterns in the SCS and showed that the currents in the Gulf were southward in fall and winter and reversed in spring and summer. The predominant responses of the circulation to the seasonal monsoon wind were also shown in many modeling studies during the last two decades (e.g., Shaw and Chao 1994; Wu et al. 1998; Chu et al. 1998; Xue et al. 2004; Gan et al. 2006; Chern et al. 2010). Using the monthly averaged climatological wind, Shaw and Chao (1994) revealed the currents at 2.5 m were southeastward and southwestward in the Gulf in August and December, respectively. In a follow-up study, Wu et al. (1998) pointed out there were seasonal and inter-annual variations of the circulation. Also using the climatological monthly mean wind, Xue et al. (2004) showed the annual evolution of the circulation in the SCS. With a horizontal resolution of ~ 10 km for the northern shelf, the vertically averaged flows in the Gulf varies from an

Responsible Editor: Takuji Waseda

This article is part of the Topical Collection on the *4th International Workshop on Modelling the Ocean in Yokohama, Japan 21–24 May 2012*

J. Gao · M. Shi
Ocean University of China, Songling Road 238, Qingdao, China

J. Gao · H. Xue (✉) · F. Chai
School of Marine Sciences, University of Maine, Orono,
ME 04469-5706, USA
e-mail: hxue@maine.edu

J. Gao
Guangxi Academy of Sciences, Daling Road 98, Nanning,
Guangxi, China

open cyclonic circulation in fall and winter to an open anticyclonic circulation from late spring to summer.

However, the models mentioned above are insufficient to reveal the detailed circulation characteristics in the Gulf. Studies specifically targeting the Gulf are needed. The first systematic survey of the Gulf was the joint program conducted by China and Vietnam in the early 1960s (Su and Yuan 2005), which indicated the circulation was unclosed anti-cyclonic and cyclonic in the summer and winter, respectively. Years elapsed until the work by Liu and Yu (1980), and after that, many studies were conducted about the tide and tidal currents in the Gulf (Li 1986; Liu and Zhang 1997; Xia et al. 1997; Wu et al. 2003). It was concluded that the diurnal tidal constituents O1 and K1 dominate in the Gulf, with M2 playing the secondary role. In addition, strong tidal currents were found in the Qiongzhou Strait (QS) and off the western coast of the Hainan Island (Hu et al. 2003). Li (1987) and Cao and Fang (1990) examined the tidally induced residual current, and the magnitude was found to be $\sim 5 \text{ cm s}^{-1}$. According to a diagnostic model, Xia et al. (1997) pointed out the circulation in the Gulf was cyclonic all year round. However, Sun et al. (2001) revealed the circulation was unclosed anti-cyclonic in summer, and the wind was the most important driving force in the Gulf. The wind-driven effect was confirmed by Manh and Yanagi (2000), who indicated the residual flow in the upper level was basically eastward or northeastward in summer and reversed in winter. On the other hand, Xia et al. (1997) and Zu (2005) concluded the circulation was cyclonic in summer mainly resulted from the density-driven residual current. Wu et al. (2008) also thought the summer circulation was anti-cyclonic due to the strong positive vorticity input from QS. Thus, the summertime circulation pattern in the Gulf remains to be controversial. Although most papers agreed on the cyclonic

gyre in winter, when and how seasonal transitions take place remain largely unknown. As well, the Gulf is connected with neighboring seas via a wide opening in the south and the QS in the east, and it also receives considerable discharges from several rivers including the Red River. How these in- and out-fluxes modify the circulation patterns needs to be examined. Lastly, seasonal evolution of water masses in the Gulf has not been studied in the previous models.

In this study, a high-resolution prognostic model simulation is conducted for 2006 and 2007, forced with tidal harmonics, daily wind, heat flux, and lateral flux, as well as climatological monthly river discharges. The rest of the paper is organized as follows: “Section 2” describes the model setup; “Section 3” describes the seasonal circulation and particularly the flows in the QS; “Section 4” discusses the seasonal evolution of water masses; and “Section 5” summarizes the main findings of this study.

2 Model setup

In this study, the circulation between 2006 and 2007 in the Gulf is simulated using the Princeton Ocean Model (Blumberg and Mellor 1987), which is a three-dimensional numerical model solving the primitive equations with free surface and 2.5 level turbulence closure (Mellor and Yamada 1982). The model domain is shown in Fig. 1, which is discretized into a total of 399×399 horizontal grids in an orthogonal curvilinear coordinate. The horizontal resolution varies from $\sim 0.9 \text{ km}$ to $\sim 2 \text{ km}$, and there are 21 sigma levels in the vertical. The depth field in the domain is derived from ETOPO2v2 (<http://www.ngdc.noaa.gov/mgg/global/etopo2.html>), with a minimum depth of 10 m. The

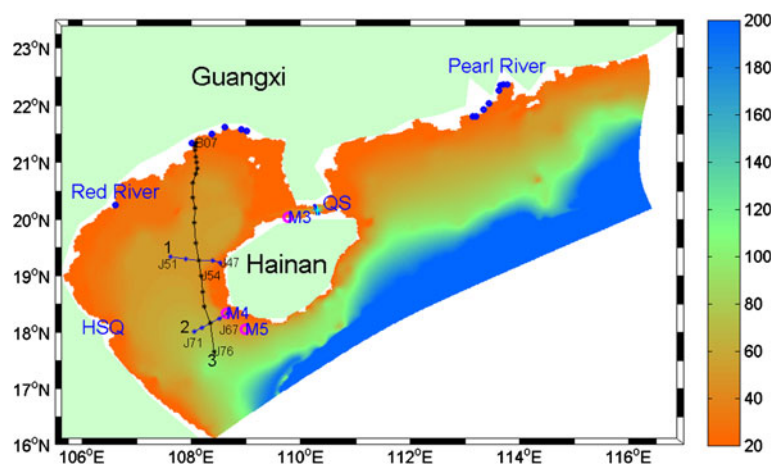


Fig. 1 Model domain and the bathymetry (colored field, unit: meters) from ETOPO2v2. Depths greater than 200 m are shown as one color. Blue dots represent the river runoffs entering the northwestern SCS. QS is the Qiongzhou Strait, and HSQ represents Cape Hoanh Son Quan. In situ observations in 2007 from “cross sections 1, 2 and 3” as well as

moorings M3–5 (magenta circles) are used to compare with the model results. The blue line in the QS represents the section utilized to calculate the zonal flux in “Section 3,” with the blue star representing the station where the velocity profiles are extracted and shown in Fig. 10

maximum depth in the domain is 2,129 m on the southeastern side of the domain.

For the surface forcing, the daily averaged blended wind (<http://www.ncdc.noaa.gov/oa/rsad/air-sea/seawinds.html>) is used, which is a product merged from multiple satellite scatterometers and model analysis on a global 0.25° grid (Zhang et al. 2006). In addition, the daily averaged heat flux is obtained from the OAFflux Project (<http://oafux.who.edu/descriptionheatflux.html>), which represents the best possible estimate on a global 1° grid, synthesizing measurements from various sources (Yu et al. 2008). In this model, no precipitation and evaporation are considered.

The Pearl River with a climatological annual mean discharge rate at about 10,300 m³s⁻¹ is by far the largest fresh water source to the region. Using the seasonal distribution given by Xue et al. (2004), the resultant monthly discharges for the Pearl River are shown in Table 1. The Pearl River has important impacts on the hydrography and flow regimes in the northern SCS (Xue et al. 2004; Gan et al. 2009), but the Pearl River is more than 200 km east of the Gulf, so that only its peripheral effect reaches the Gulf via the QS. In this study, the Pearl River discharge is divided into eight branches as in Xue and Chai (2002) and Wong et al. (2003). The percentages for individual branches from the west to the east (see Fig. 1) are 6.0, 6.2, 6.1, 28.3, 11.2, 6.4, 17.3, and 18.5, respectively (Xue and Chai 2002). The second largest discharge comes from the Red River, and its climatological monthly discharge (see Table 1) is adopted from Van Maren and Hoekstra (2004). Six additional rivers located at the northern coast of the Gulf (Guangxi Province, China) are also considered in the model.

Due to the strong tidal mixing in the domain (Shi et al. 2002; Hu et al. 2003; Lu et al. 2008), six principal tidal constituents (K_1 , O_1 , P_1 , M_2 , S_2 , and N_2) are prescribed at the two open boundaries. The tidal constants are derived from the Oregon State University tidal model (<http://volkov.oce.orst.edu/tides/YS.html>), which has a horizontal resolution of 1/30° in the

China Seas with the root mean square error of K_1 and M_2 being 1.63 and 4.16 cm, respectively (Zu et al. 2008).

In addition, daily averaged elevation, temperature, salinity, and barotropic (vertically averaged) and baroclinic velocities obtained from the global 1/12° HYCOM+NCODA analysis between 1 December 2005 and 31 December 2007 are specified at the two open boundaries. As in Xue et al. (2004), Flather (1976) boundary condition is applied to relate the barotropic velocity and the elevation; gravity wave radiation combined with three-point smoothing is applied to the baroclinic velocity; and upwind advection is adopted for the temperature and salinity.

The model is spun up from the temperature and salinity of 1 December 2005 from the HYCOM+NCODA with zero elevation and velocities. The time steps of internal mode (baroclinic) and external mode (barotropic) are set to 20 and 1 s, respectively. The daily averaged results after 1 March 2006 are analyzed.

3 The circulation

The monthly mean circulation for January and July of 2007 are shown in Fig. 2. There appeared a current that traversed the Gulf from HSQ to QS to separate the Gulf into the northern and southern basin. This current was southwestward in January (Fig. 2a) but reversed to northeastward in July (Fig. 2b), consistent with the monsoon wind directions. In the southern Gulf, the circulation was cyclonic in January but turned to anti-cyclonic in July. In January, there was a southwestward current on the shelf and slope in the SCS, most of which turned southward and bypassed the Gulf. However, the shelf portion separated into several branches as it rounded the corner of the Hainan Island. The northern most branch flew northwestward into the southern Gulf, and it joined the southwestward current from the QS to move westward across the Gulf at ~18.5°N. The joined current

Table 1 Climatological monthly discharges of the major rivers in the northwestern SCS

Rivers	Monthly discharge (10 ⁸ m ³)											
	1	2	3	4	5	6	7	8	9	10	11	12
Pearl	94.5	91.3	110.8	228.2	453.1	446.6	560.7	469.4	299.9	218.4	157.3	127.1
Nanliu	1.50	1.64	1.91	5.39	6.27	11.5	10.5	14.4	7.30	3.55	2.59	1.71
Qin	0.37	0.33	0.49	1.22	1.67	3.49	3.76	4.27	1.86	0.96	0.71	0.47
Fangcheng	0.34	0.35	0.48	0.78	1.42	2.51	4.11	3.49	2.00	1.08	0.73	0.43
Dafeng	0.22	0.20	0.28	1.06	1.43	3.42	3.93	4.46	1.79	0.75	0.48	0.28
Maoling	1.06	0.90	1.10	2.31	2.65	3.53	4.43	4.93	4.06	2.23	1.04	0.78
Beilun	0.62	0.62	1.00	1.66	3.32	4.48	6.54	5.12	2.82	1.78	0.83	0.54
Red	6.53	6.53	6.53	6.53	7.62	16.3	32.6	49.0	42.5	30.0	19.1	11.4

formed the western limb of the cyclonic circulation and flew southward off the Vietnamese coast. Two other branches flew westward across the mouth of the Gulf to join the aforementioned southward flow and eventually exit the Gulf along the Vietnamese shelf. In summer, the upper layer circulation in the SCS reversed, and the current was northward along the Vietnamese coast as seen in Xue et al. (2004), which penetrated into the southern Gulf to drive an anti-cyclonic circulation in July (Fig. 2b). Furthermore, the near-shore flow separated from the coast at HSQ to form the current traversing the Gulf that eventually exited the Gulf from the QS.

Flow patterns were more complex in the northern Gulf. In January, the northern Gulf appeared to have a cyclonic circulation in the west, which was separated from an anti-cyclonic lobe in the east, whereas in July flows were mostly eastward in the west and there was a cyclonic lobe in the northeast. The sea level was higher in January, especially along the Vietnamese coast resulted from the water pile-up under the northeasterly monsoon. The spatially averaged elevation in the Gulf was ~ 0.9 m in January, about 30 cm higher than that in July.

Separation of the circulation into the southern and northern Gulf is further substantiated in Fig. 3 that shows the flow patterns at the surface and 40 m depth, respectively. Driven by the winter monsoon, surface flows in January were mostly west- and southwestward, while at 40 m flows were northeastward in the northern Gulf (i.e., opposite to the flows at the surface) in contrast to the cyclonic circulation in the southern Gulf. In July, the anti-cyclonic circulation was most obvious at depth in the southern Gulf, but the anti-cyclonic

tendency was also evident at the surface. In the northern Gulf, flows were mostly east- and northeastward both at the surface and at 40 m but much weaker at 40 m.

3.1 Seasonal transition of the circulation

To understand how the wind drives the seasonal transition of the circulation, the gulf-wide averaged wind and the associated low-pass signal are shown in Fig. 4. Although the model was driven by spatially variable wind, the difference in wind conditions across the Gulf (from the blended wind at 0.25° resolution) was small except in a few occasions when a tropical storm passed the middle of the Gulf. The low-pass Lanczos filter used in this study had a cutoff period of 80 days, which was selected so that the low-passed time series and the remnant could maintain the annual and synoptic frequency peak, respectively. The filtered time series show that monsoon wind was southwesterly in boreal summer (from May to July) and northeasterly in fall and winter (from September to February), respectively (Fig. 4b). The transition from southwesterly to northeasterly appeared in late August in 2006, which was earlier than in 2007 because there were several tropical cyclones across the northern SCS and the Gulf in August 2006. These events had significant effects on the flows through the QS as seen in “Section 3.3.”

Unlike the wind, complex spatial patterns emerged from the circulation in the Gulf, for which the low-pass currents in four quadrants of the Gulf (see Fig. 2 for their locations) are shown in Fig. 5 to illustrate the seasonal evolution in 2006 and 2007 and the relationship to wind forcing. The low-pass

Fig. 2 Vertically averaged velocity and elevation (meters) for January (a) and July (b) 2007. Low-pass-filtered, areal averaged velocities in boxes 1–4 are used in Fig. 5 to describe the seasonal evolution of currents in the four quadrants of the Gulf

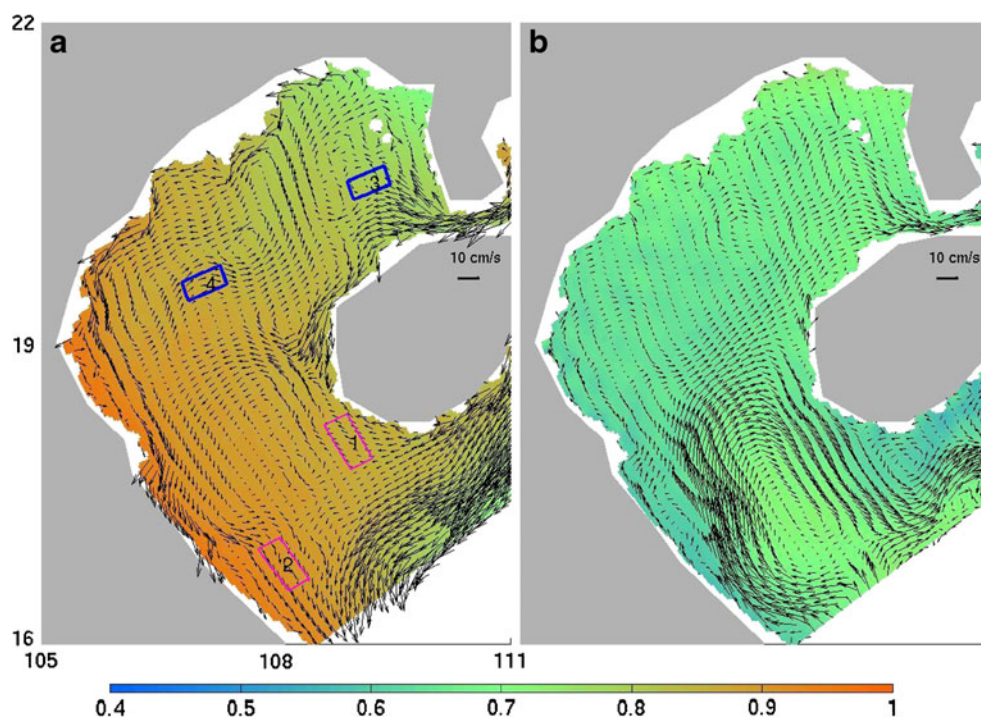
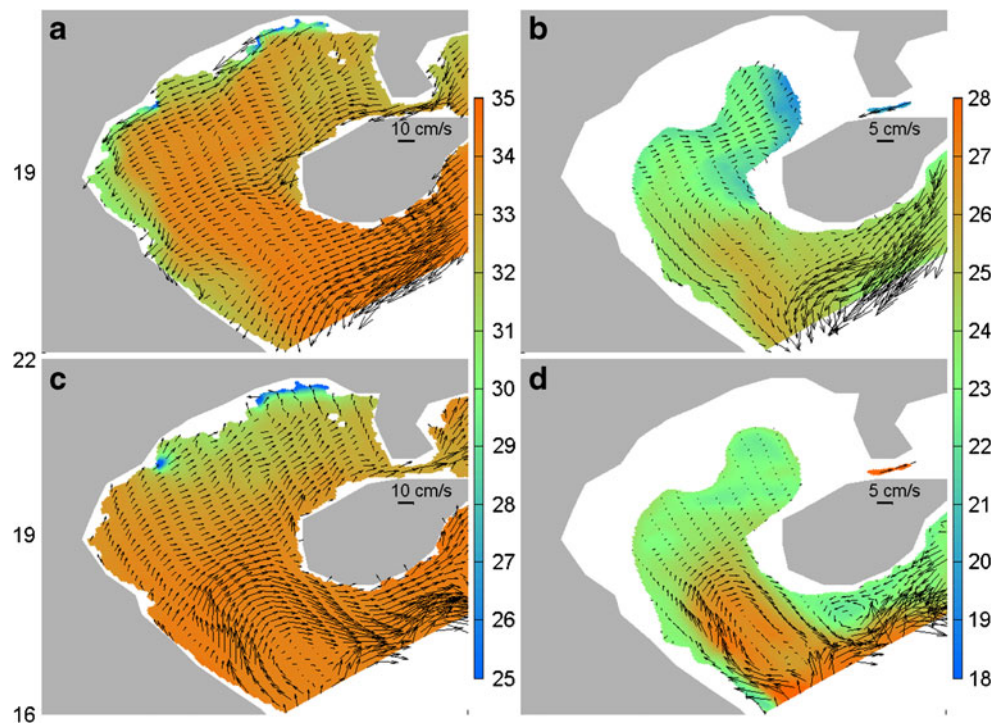


Fig. 3 The velocity and salinity at the surface (**a** and **c**) as well as the velocity and temperature (degrees Centigrade) at 40 m (**b** and **d**) in January (**a** and **b**) and July (**c** and **d**) of 2007



vertically averaged velocities appeared to be stronger in box 2 (Fig. 5b) than those in box 1 (Fig. 5a), but they had the vector correlation coefficient (Crosby et al. 1993) at 0.84 and component Pearson coefficient R at $-0.9/-0.8$ for the zonal

and meridional currents, respectively. The correlations imply a coherent gyre in the southern Gulf with box 1 and 2 being on the opposite sides of the gyre as seen in Fig. 2. The gyre was also highly correlated to the annual cycle of the wind

Fig. 4 Spatially averaged zonal (green) and meridional (blue) winds in the Gulf from March 2006 to December 2007. **a, b** The original and lowpass filtered time series, respectively. All units are in meters per second

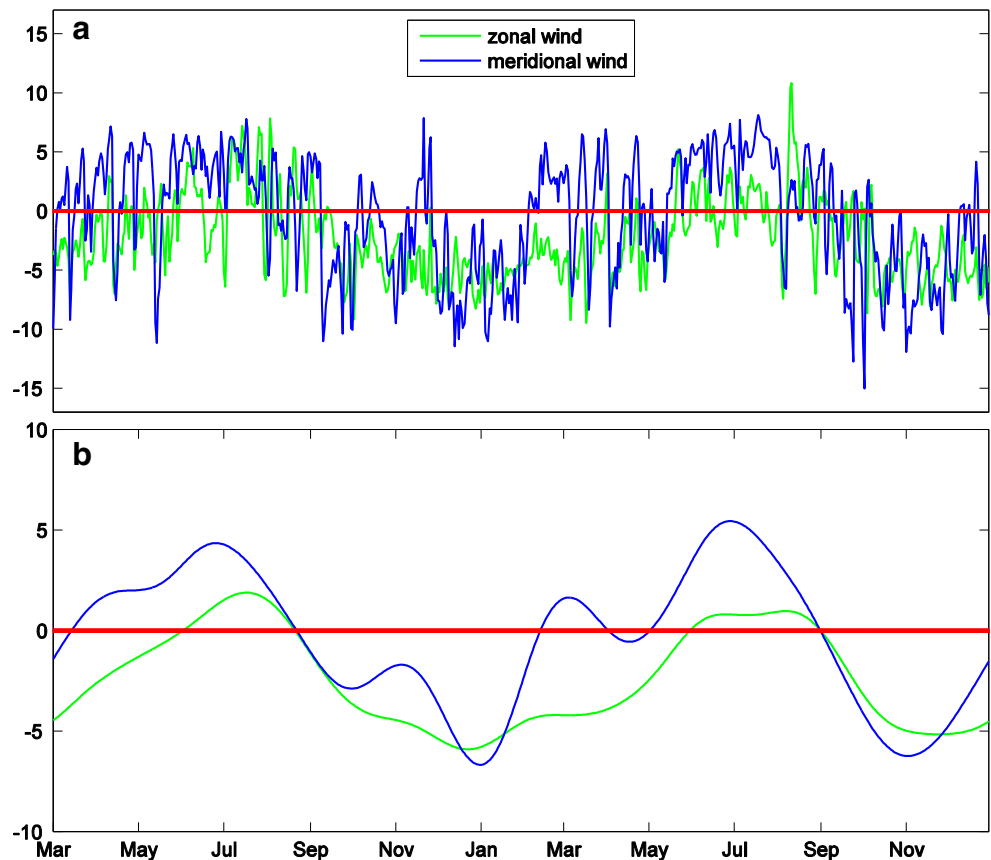
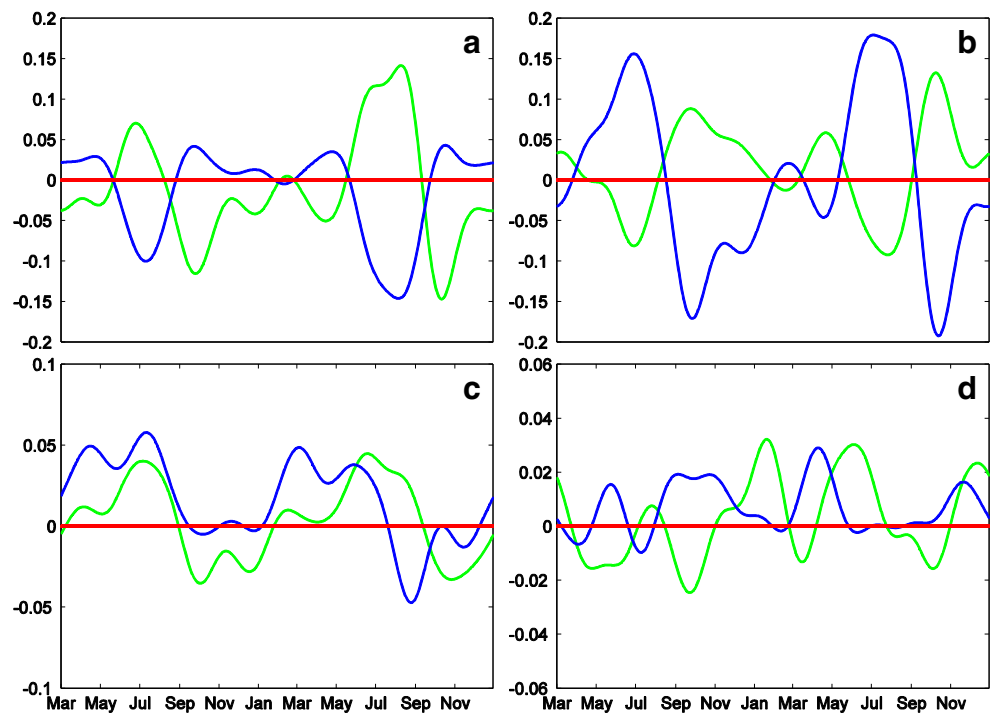


Fig. 5 Low-pass-filtered areal averaged currents in boxes 1–4 (a–d, see Fig. 2 for locations of the boxes) from March 2006 to December 2007. Blue/green curves represent meridional/zonal currents, respectively. All units are in meters per second



with the vector correlation coefficient between the current and the wind at 1.1 and 0.8 in boxes 1 and 2, respectively. The circulation was cyclonic from September till April the following year, whereas it was anticyclonic from about May to August. The flows in both boxes were two to three times stronger in the summer and fall, although the wind was generally stronger in the winter.

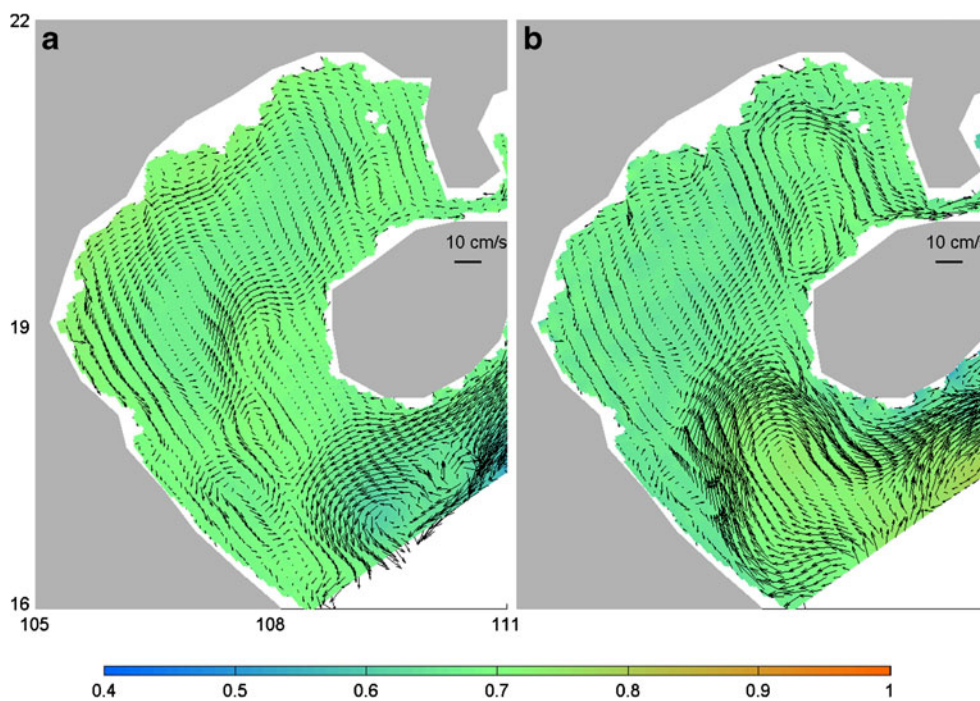
The low-pass velocities in the northern Gulf, less than 7 cm s^{-1} in box 3 and 4 cm s^{-1} in box 4 (Fig. 5c and d), were weaker than those in the southern Gulf. Flows in box 3, which appeared to be connected with that in the QS (see Fig. 2), still had apparent annual cycle, being mainly northeastward in spring and summer but westward in fall and winter (Fig. 5c). A strong southeastward flow occurred in July and August 2007, in contrast to the northeastward flow during the same months in 2006. This difference was caused by more frequent westward flows through the QS in August 2006 (see Figs. 9 and 10 in “Section 3.3”) that deflected the northeastward current originated off the Vietnamese coast to pass box 3 (Fig. 6a). Furthermore, in the model, an anticyclonic eddy developed off the northwest corner of the Hainan Island that steered the northeastward current originated off the Vietnamese coast northward, so that one branch could reach at $(108^\circ\text{E}, 21^\circ\text{N})$, which then turned southeastward to pass box 3 in July and August 2007 (Figs. 2b and 6b). Flows in box 4 lacked the apparent annual cycle (Fig. 5d). The meridional current was mainly northward except in March–April and July of 2006, while the zonal current was eastward in March and July 2006, from November 2006 to February 2007, and from April through July in 2007. The eastward flow in January appeared to be related to the eastward flow at depth

(see Fig. 3a, b) while in July it was primarily from the wind-driven flow at the surface (see Fig. 3c, d). The westward zonal flows from April through June and from late August through October in 2006 as well as in March and August through October in 2007 were mainly influenced by the northwestward current off the western coast of Hainan as the cyclonic circulation in the southern Gulf intruded further north into the Gulf (not shown).

The vector correlation coefficient was only 0.33 between the low-passed currents in boxes 3 and 4, auguring again for separated flow features in the northeastern and northwestern parts of the Gulf (see also Fig. 2). The low-passed currents in box 3 were highly correlated to the wind with the vector correlation coefficient = 1.1. Moreover, the northeastern Gulf was also strongly affected by seasonal flows in the QS (see more discussion later in “Section 3.3”). On the contrary, the interior of the northwestern Gulf was affected by several currents, including the southward/northward current off the Vietnamese coast in winter/summer, which fed the flows traversing the Gulf between HSQ and the QS (Fig. 2), the northwestward current off the western coast of Hainan (fed by the cyclonic circulation in the southern Gulf and occurred in September and October), and the southwestward current off the northern coast of Hainan (fed by the westward current from the QS in fall and winter). Consequently, the low-passed current had no apparent annual cycle (Fig. 5d), and the correlation with the low-passed wind was low in box 4 with the vector correlation coefficient = 0.3.

To distinguish the effect of local wind from the remote forcing, another experiment with no local wind was carried out. Although the run did not finish the second year integration

Fig. 6 Vertically averaged velocity and elevation (meters) for August 2006 (a) and August 2007 (b)



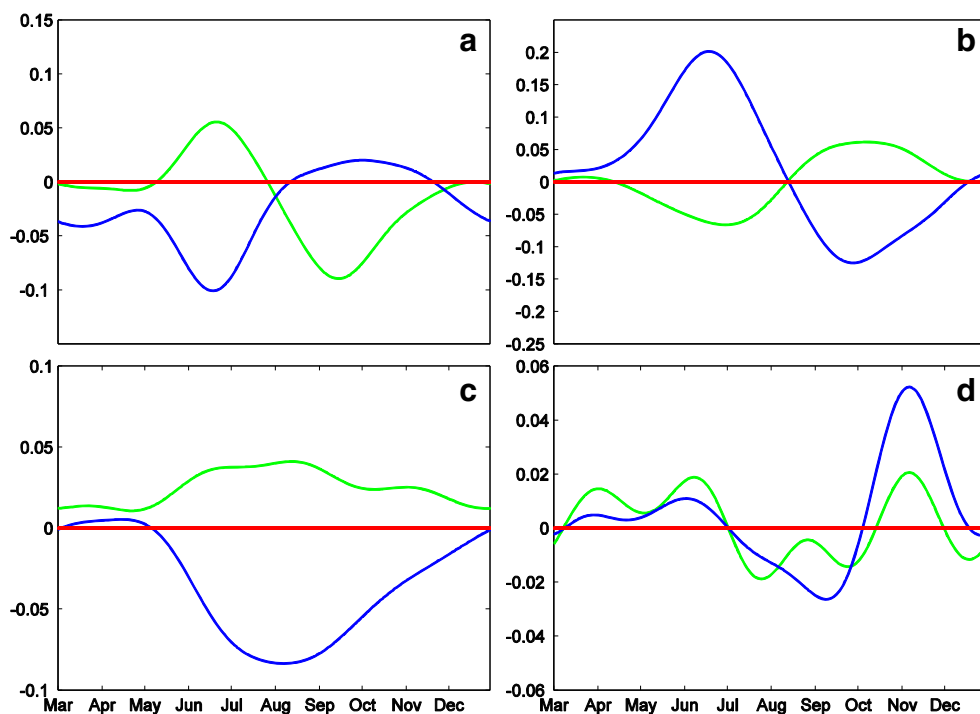
due to the mismatch between the surface forcing and the open boundary condition, time series of the low-pass filtered velocities in 2006 show a seasonal evolution in the southern Gulf (Fig. 7a, b) that was similar to the time variation in the base experiment (see Fig. 5a, b), but the differences were rather significant in the northern Gulf between the experiment without the local wind forcing (Fig. 7c, d) and the base experiment (see Fig. 5c, d). This suggests that the remote forcing via the currents through the open boundaries played a more significant

role in driving the southern gyre, while the local wind forcing was more important in the northern Gulf.

3.2 Currents Southwest of Hainan

The discussions above suggest that the current off the southwestern coast of Hainan was not only an indicator of the circulation in the southern Gulf but also played a role in affecting the circulation in the northwestern Gulf. In addition

Fig. 7 Similar to Fig. 5 but for the experiment without the local wind forcing from March to December 2006 only



to the seasonal variability seen from the flows in box 1 (Fig. 5a), direct observations of currents from two moorings southwest of the Hainan Island (M4 and M5) were obtained from April to May in 2007 (Wang et al. 2008). At M4, the current was mostly westward except in the bottom 5 m where the current reversed, whereas at M5 the current was south-westward at 5 m from the surface and rotated counterclockwise with the depth until the lower part of the bottom boundary layer. These features were produced favorably in the model, and the model suggested stronger currents in the upper few meters where the direct observations were not available (Fig. 8). However, the rotation of the current at M5 in the model was not as strong as the observed. Other than the deeper water depth at M5 where both the surface and bottom Ekman layers were more likely to develop independently (Durski et al. 2004), small-scale, localized features or processes, e.g., a topographic bump, might contribute to the stronger flows in the bottom boundary layer observed at M5. Without such features in the model, the bottom boundary layer was rather similar between stations M4 and M5.

3.3 Flows in the QS

The QS represents the sole conduit between the Gulf and the Guangdong coast to the east. It was generally agreed that the flows in the QS are westward in winter. However, the main discrepancy from previous studies (e.g., Shi et al. 2002; Xue et al. 2004; Chen et al. 2009) is whether the flows remain westward in summer. Current profiles at M3 near the western

entrance of the QS (see Fig. 1 for the location) were measured using an Acoustic Doppler Current Profiler from 23 July to 24 August 2006 (Zhang et al. 2008), which showed the current was eastward in late July and strongly variable in August. In the model, flows at M3 (see Fig. 9b) were generally eastward till 28th of July, then turned westward at all vertical levels between 29 July and 2 August, followed by an extended period of generally eastward flows till 21 August except for the brief reversals in the top 10 m or so on 5, 10, 11, and 14 August. From 21 to 24 August, the flows were again westward, almost the entire water column on 21st and 24th but only in the top 7 m on 22nd and 23rd. The variations were in qualitative agreement with the observations obtained by Zhang et al. (2008), especially for the zonal current, although the timing was sometimes off by a day.

However, the correlation between the current and the local wind at station M3 was low with $R=0.4/0.3$ between the zonal current and the meridional/zonal wind, respectively (the meridional current was far less than the zonal current because of the coastline orientation near M3). For instance, although there was stronger easterly wind between 12 and 15 August, the westward current was weaker than that in the period of 10 and 11 August. On the other hand, the sea level difference between the eastern and western sides of QS (Fig. 9a) was found to affect more strongly on the zonal current with $R=0.55$.

Throughout the simulation period, flows in the QS were mostly east- and westward, aligning with the direction of the strait with the zonal flows reaching about five times that of

Fig. 8 Observed and modeled velocity profiles at stations M4 (left) and M5 (right), averaged from 17 April to 17 May in 2007

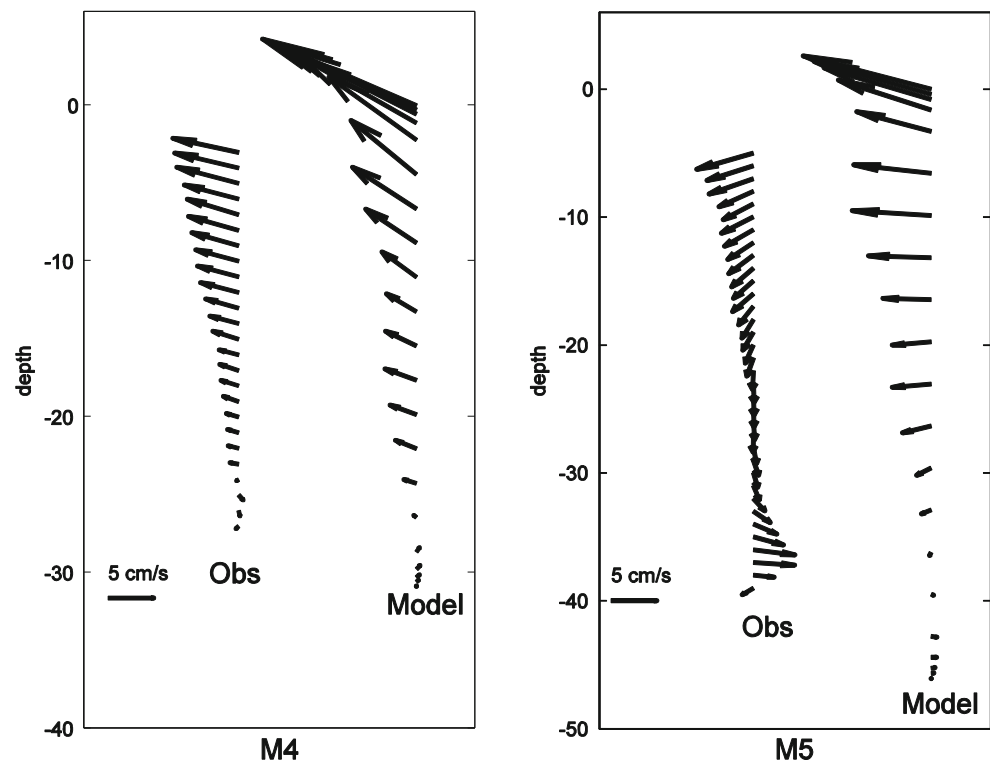
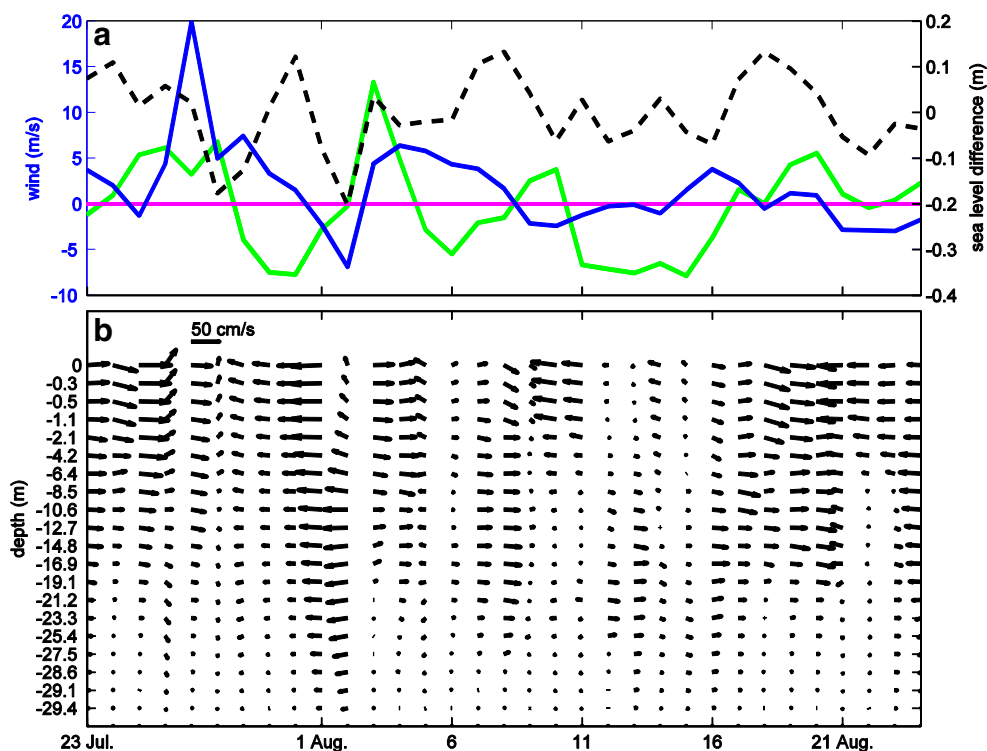


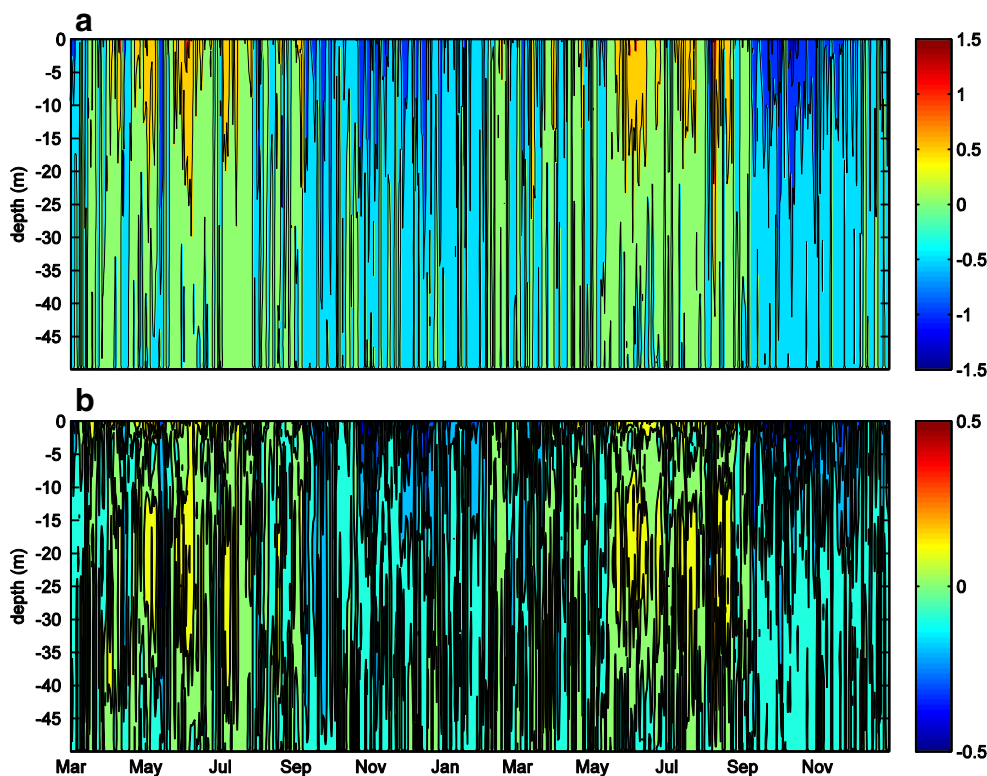
Fig. 9 **a** The zonal (green) and meridional wind (blue) at station M3 during the same period, with the black dashed line representing the sea level difference between the eastern and western end of the QS. **b** The model predicted daily averaged current profiles at station M3 from 23 July to 24 August 2006. Arrows pointing up and right represent northward and eastward flows, respectively



the flows across the strait (Fig. 10). Flows were generally westward from August 2006 to April 2007 and September 2007 till the end of simulation. Turning to eastward occurred in late March 2006 but delayed till mid-April in 2007. The flow direction was generally consistent in the vertical, but

the zonal flows were stronger near the surface while the meridional flows were stronger in the mid water column especially in summer months. There were periods in both summers with the eastward zonal flow exceeding 0.50 cm s^{-1} (namely, early May, June, and July in 2006 as well as late

Fig. 10 Time series of the zonal (a) and meridional (b) velocity profiles in the QS (see the blue star in Fig. 1) from the model. Units are in meters per second



May, early July and mid-August in 2007). These events were also manifested in the meridional current as strong northward flows in the mid-water column. In between these eastward flows, there were pulses of southwestward flows (e.g., mid-May, early July, and multiple times in August 2006, as well as one occasion in early August 2007) with the westward current exceeding 0.5 m s^{-1} from the surface down to 35 m depth. These pulses of southwestward flows were induced by tropical cyclones passing east of the Hainan Island. The cyclones in May 2006 and August 2007 were close enough to be seen as the spiked northeasterly wind in Fig. 4a. On the other hand, the storm in early August 2006, not a strong event in Fig. 4a, was further to the east with the storm center passing near 113.25° E . The strong westward current in the QS during this event was mainly induced by the water piling-up east of the Leizhou Peninsula and Hainan Island resulted from the storm.

Although the tidal induced residual current was westward all year round (Shi et al. 2002), the daily averaged current in the QS had strong variations adjusted by not only the local wind but also the wind driven sea-level difference. Shi et al. (2002) pointed out the volume transport through the strait was important to the Gulf and the westward flux was $\sim 0.2\text{--}0.4 \text{ Sv}$ in fall and winter. The present model result estimated that the averaged westward flux was $\sim 0.35 \text{ Sv}$ in fall and winter contrasting to the mean eastward flux of $\sim 0.25 \text{ Sv}$ between May and July. The yearly averaged flux was westward through the QS at $\sim 0.1 \text{ Sv}$, which was equivalent to a net renewal of 41 % of the total Gulf volume on the yearly basis.

In summary, because the variability was at least as strong as the seasonal current, flows in the QS could be eastward or westward at any given day in summer or winter, but the seasonal mean currents were eastward between late spring and summer and westward during the rest of the year. There had been other circumstantial evidences to support the presence of eastward flows in the QS during the summer. For example, historical observations of drift bottles showed five out of the eleven bottles released in June and July between 1964 and 1969 from the western end of the strait ended near the eastern end, but the other six ended inside the Gulf near the northern coast (from Shi, unpublished data). Another evidence was the observed salinity from 1960s (Table 2), which showed that the saline water ($\sim 34\text{‰}$) was found in the QS from May (except at 0 m) to August. Since the discharges from the Pearl River in summer months are higher (Table 1),

the corresponding salinity off the southeastern Guangdong coast is $<33\text{‰}$ (Yang et al. 2003). A plausible explanation would be a northwestward saline current separated from the northeastward current off the eastern coast of Hainan in summer. However, there was no evidence to support this branch under the southwesterly wind (Hu et al. 2000; Yang et al. 2003; Liu et al. 2008). Therefore, the saline water in the QS was most likely to be brought from the Gulf by the eastward current in summer (Fig. 3c), which was from the northward saline water off the western coast of Hainan, originated from the southern SCS. The sudden increase of salinity from $\sim 30\text{‰}$ in April to $\sim 34\text{‰}$ in May indicated the transition of the current from westward to eastward. From August to September, the salinity was reduced by $\sim 1.5\text{‰}$ when the less saline water from the Guangdong coast was pushed into the strait by the northeasterly wind. As the discharge from the Pearl River weakened from October to November, the salinity in the QS increased again.

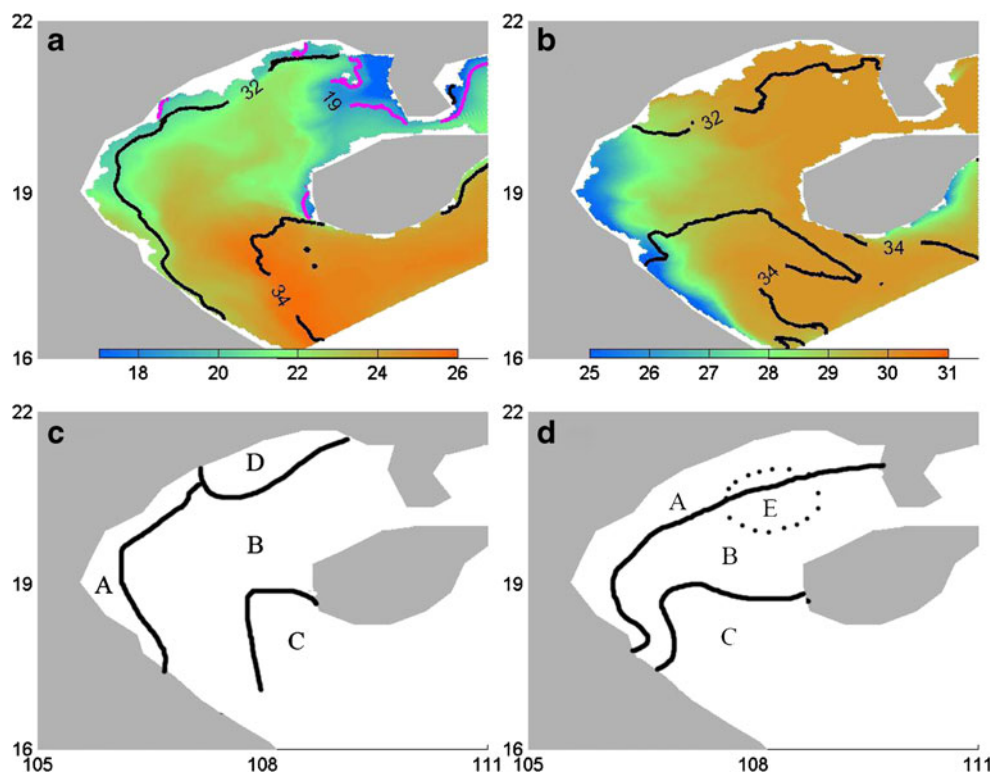
4 Water masses

Similar to the circulation, water masses in the gulf exhibited seasonal variations as well. In winter, the SCS water ($S \geq 34\text{‰}$) penetrated into the southern Gulf off the coast of Hainan as the eastern limb of the cyclonic gyre (Fig. 11a). The southward Red River plume, seen as the low salinity water (also schematically as water mass A in Fig. 11c), contributed to the western limb of the cyclonic gyre. Because the prevailing northeasterly wind was downwelling favorable, the low salinity coastal water was pushed close to shore. Moreover, the river plumes along the Guangxi coast in the northern Gulf could be distinguished for its low temperature ($<19^\circ \text{C}$, also as the cold water mass D in Fig. 11c). Between the coastal waters and the SCS water, the gulf water (the water mass B) was a mixture of the low-salinity coastal water masses and the saline water from the SCS. In summer, the hot and saline SCS water (water mass C) intruded into the southern Gulf off the Vietnamese coast. As it met the mixed gulf water (water mass B), it turned anti-cyclonically and flew out of the Gulf on the Hainan side (Fig. 11b). Water mass D disappeared in summer because of relatively uniform warming throughout the gulf. Furthermore, the upwelling favorable southwesterly monsoon wind caused the coastal water mass A to spread further eastward and offshore at the surface. The modeled water characteristics

Table 2 Monthly averaged salinity derived from the observations collected at 111° E and 20.3° N near the eastern end of the QS in 1964 and 1965

Depth	Mar	Apr	May	Jun	Jul	Aug	Sept	Oct	Nov
0 m	32.64	30.35	29.88	33.78	33.29	32.89	31.33	33.07	33.73
10 m	32.69	30.72	34.17	34.29	33.49	33.86	31.48	33.17	33.69
20 m	33.03	31.37	34.34	34.49	34.60	33.97	32.20	33.47	33.76

Fig. 11 Surface salinity (*black curves*) and temperature (*color and pink curves*) in January (a) and July (b) of 2007 from the model. Sketches of water masses in the Gulf in winter (c) and summer (d) based on the Joint Survey conducted by China and Vietnam in 1964 and 1965 (Shi, unpublished). The *solid lines* in (c) and (d) delineate the separation between surface water masses, whereas the *dashed ellipse* represents a distinct cold water mass at depths



along the Vietnamese coast in July 2007 was rather different from the sketch based on the Joint Survey in 1960s (Fig. 11d), which was conducted during a period of calm wind. As the southwesterly wind relaxed, the upwelling ceased and the Red River plume turned southward.

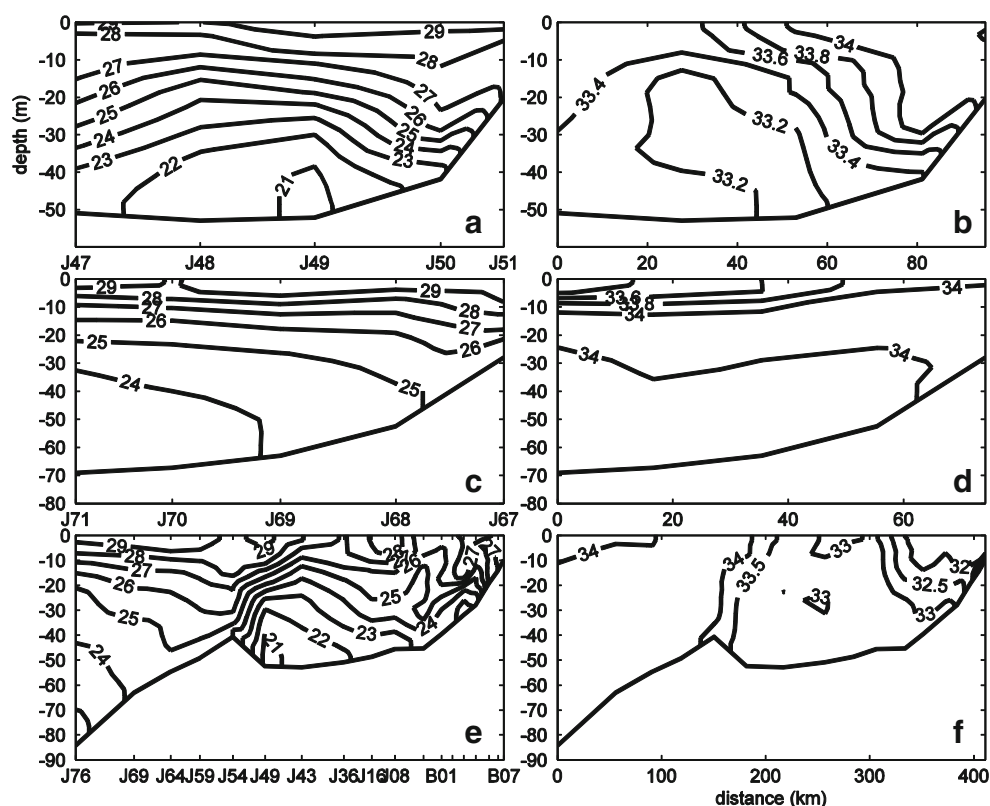
The subsurface, cold, water mass in the northern Gulf (water mass E in Fig. 11d) was found not only during 1960s but also during the field survey in April 2007. Huang et al. (2008) showed that there was a cold and fresh water mass at “cross-section 1” (see Fig. 1 for the location) below 30 m with the core being less than 22 °C. This cold water mass was also present in the model at station J49 with the core temperature <21 °C (Fig. 12a, e). The hot and saline water from the SCS moved northward along the west coast of the Hainan Island so that there were strong lateral gradients of temperature and salinity. The salinity at “cross-section 1” was higher in the upper layer (Fig. 12b). On the contrary, the salinity at “cross-section 2” increased from the surface to about 20 m but without much gradient below 20 m (Fig. 12d). The temperature decreased with depth, and the thermocline was at ~20 m at the offshore stations (J71 and 70), which tilted downward as getting closer to shore. These patterns were qualitatively similar to the result of Huang et al. (2008). However, the lateral gradient near shore was weaker in the model for both the temperature and salinity.

The difference between the two cold water masses could also be seen from “cross-section 3” (Fig. 12e, f). The fresh and cold water mass at J49 (“cross-section 1”) was separated from the cold and saline water at J69 (“cross-section 2”) by

the temperature and salinity fronts near station J54, where there is a ridge that separates the southern gulf from the northern gulf. To the south of J54, the warm and saline water from the SCS was present in the southern Gulf between J76 and J54, with a thermocline at ~10 m. Under the thermocline layer, the cold water tilted downward into the gulf. In the northern Gulf, there was a cold and fresh (<33.2‰) water dome between J54 and J08. The biggest differences between the model and the observations of Huang et al. (2008) were on the northern shelf between B01 and B07. In the model, the low salinity (<32‰) was resulted from the Beilun River plume that subducted toward station B01, which also shielded some cold water with the temperature <23 °C. In the observation, the extent of the Beilun plume was much smaller with the salinity of ~32.8‰ at B07 only, but the cold temperature near the bottom was only 18.5 °C, i.e., 4–5 °C colder than the model prediction. Because the real-time discharge was not monitored, it was not the objective of this study to hindcast the plume. Nevertheless, the complex T/S patterns were qualitatively produced in the model despite of the considerable differences in the magnitude.

The cold water masses seen at depth in April were generated in winter due to the strong mixing associated with the northeasterly monsoon wind, which produced cold waters along the northeastern coast and the Hainan coast (Fig 13a) with the former being about 2 °C colder. The formation of cold water masses especially along the northwestern coast of Hainan was aided by the cold Guangdong coastal water through the QS. By April (Fig. 13b), the surface had been

Fig. 12 The model predicted temperature (*left*, in °C) and salinity (*right*, in ‰) from “Section 1” on 26 April 2007 (**a** and **b**), from “Section 2” (**c** and **d**) and “Section 3” (**e** and **f**) on 29 April 2007. Stations J47–J51 on “Section 1”, J71–J67 on “Section 2 and J76–B07 on “Section 3” are marked in Fig. 1



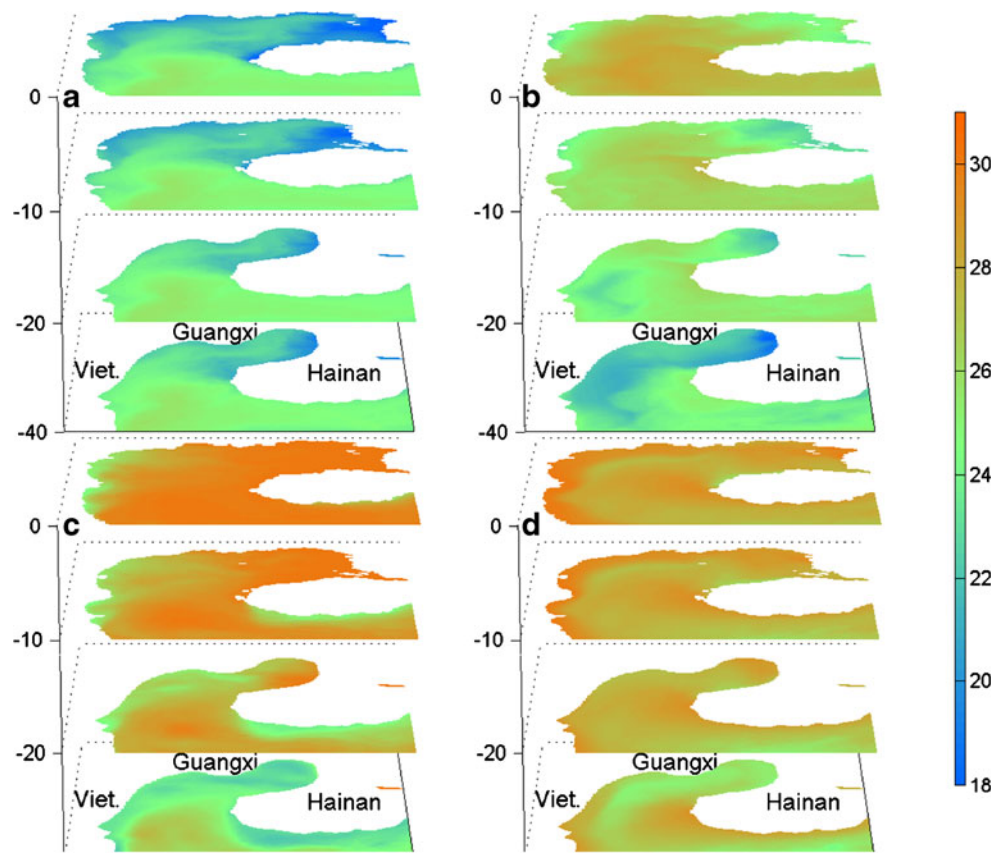
warmed up as the downward heat flux from the shortwave radiation increased and as the warm SCS water intruded the Gulf from south and west of the Hainan Island. The warming was limited to the upper water column (10–20 m deep), below which the temperature remained cold, colder in the northeastern basin than in the southern gulf as seen in Fig. 13b. Because the deep water preserved the cooling effect throughout the winter, the deep temperature was lower in April than in January. By July (Fig. 13c), the warming had penetrated deeper especially in the southern and northeastern Gulf while the northwestern shelf and the region southwest of the Hainan Island were considerably colder. The upwelling was clearly visible at the surface off the Vietnamese coast and southeast of the Hainan Island (also seen in Fig. 11b). However, the upwelling southwest of the Hainan Island was present only from 10 m down, consistent with the weak upwelling suggested by Lu et al. (2008). The surface warming continued from July to October. When the wind switched from southwesterly to northeasterly, the anticyclonic circulation transitioned gradually to the cyclonic circulation in October. Upwelling along the Vietnamese coast disappeared, which was replaced by the downwelling. As well, the area southwest of the Hainan Island was replaced by a warm water pool, which could be attributed to the orographic wind wake (Li et al. 2012). In addition, there were several intense storms in August through October (see Fig. 4), which helped to mix warm waters downward so that the deep temperature reached its maximum in October.

5 Summary

Despite being the only gulf in the northern SCS, gulf-wide hydrographic surveys were conducted in the Gulf of Tonkin only during 1960s. In situ observations using contemporary equipment were obtained in 2006 and 2007 but were limited to the eastern half of the Gulf. This study aimed to illustrate the seasonal evolutions of the circulation and water masses using a numerical model that also extrapolated the limited hydrographic observations. The model result revealed detailed circulation patterns and water mass distributions in the Gulf as follows:

1. In the southern Gulf, there was a coherent anti-cyclonic gyre in summer, which reversed to an open cyclonic circulation from fall to next spring. The eastern limb of the cyclonic gyre was supported by observations from two moorings off the southwestern coast of Hainan in April 2007. The circulation in the Gulf was highly correlated to the wind, and it was also affected by the exterior circulation from the SCS in the south and the flows from the QS in the northeast.
2. It was concluded from this study that the zonal current in the QS was several times stronger than the flows across the strait, and the seasonal mean zonal current was eastward between later spring and summer but westward in other seasons. The annual mean transport was westward

Fig. 13 The modeled temperature (unit: degrees Centigrade) at 0, 10, 20, and 40 m in January (a), April (b), July (c), and October (d) of 2007. The *x* and *y* axes represent longitude and latitude, respectively. Viet. represents Vietnam



at ~ 0.1 Sv. However, day-to-day variations were generally stronger than the seasonal mean current so that the flows could be eastward or westward in any given day, summer or winter. These results were consistent with the variability of salinity observed in the eastern end of the QS and supported by the movements of drift bottles and direct current observations in the QS. The sea level difference appeared to play a more significant role than the local wind in inducing day-to-day variations.

3. The model result also showed seasonal evolution of water masses in the Gulf. The warm and saline SCS water was found in the southern Gulf, which intruded farther into the Gulf in summer. The coastal plumes were found near the northern and western coasts of the Gulf, which extended southward past HSQ in the winter but retracted to $\sim 20^\circ$ N while spreading eastward and offshore in the summer. At lower levels, there existed two cold water masses: The colder and less saline water mass in the northern Gulf was separated from the cold and saline water mass in the southern Gulf by a submarine ridge located at about 19° N. The two water masses were produced throughout the winter, which were sheltered by a thermocline in the spring and summer. They eventually disappeared in the fall.

To analyze the control factors of the circulation and water masses, three sensitivity experiments were carried out: (1) without the wind; (2) without the heat flux; and (3) without the tide. Details of the sensitivity experiments were discussed in Gao (2013). To summarize, the circulation in the Gulf was strongly influenced by the local wind, especially in the northern Gulf. The anti-cyclonic circulation in the southern Gulf remained the same, but the flows were reversed in the northern Gulf as well as along the southern coast of the Hainan Island when the local wind was turned off. In winter, the only similarity was the southwestward flows outside the Gulf along the continental slope, while the interior circulation was drastically different. Without the local wind, flows were reversed in the QS and the systematic cyclonic coastal current disappeared, which was replaced by many eddies in the interior Gulf. In contrast, there were only minor quantitative differences in the circulation when the heat flux or the tide was excluded, but the cold water masses disappeared in the experiment without the heat flux.

Although the present model qualitatively reproduced many observed features, quantitative assessment needs to be established when in situ observations become readily available. Because the Gulf is a shallow shelf sea, topographic control on the circulation can be strong. Zu (2005) pointed out that the tidally induced residual current would be totally

changed if the bottom of Gulf were flat. How the topography modulates the wind-driven circulation especially regarding to the variability in the QS should be examined in the future. Moreover, river plumes and their effects on the gulf-wide circulation should be carefully examined.

Acknowledgments This work was supported by the Program for New Century Excellent Talents in University (NECT-07-0781), the National Basic Research Program of China (No. 2011CB403500), and Guangxi Natural Science Foundation (No. 2012GXNSFEA053001). It was also supported by the program of “Construction of prognostic system for circulation in Beibu Gulf and application for pollution transport.” We thank the three anonymous reviewers for their thorough evaluation and constructive comments.

References

- Blumberg AF, Mellor GL (1987) A description of a three-dimensional coastal ocean circulation model. In: Heaps N (ed) Three-dimensional coastal ocean models. Coastal estuarine stud, vol 4. AGU, Washington, D. C, pp 1–16
- Cao DM, Fang GH (1990) A numerical model of the tides and tidal currents in Beibu Bay. *Chin J Oceanol Limnol* 21(2):105–113 (in Chinese with English abstract)
- Chen CL, Li PL, Shi MC, Zuo JC, Chen MX, Sun HP (2009) Numerical study of the tides and residual currents in the Qiongzhou Strait. *Chin J Oceanol Limnol* 27(4):931–942
- Chern C-S, Sen J, Wang J (2010) Numerical study of mean flow patterns in the South China Sea and the Luzon Strait. *Ocean Dyn*. doi:10.1007/s10236-010-0305-3
- Chu PC, Chen YC, Lu SH (1998) Wind-driven South China Sea deep basin warm-core/cool-core eddies. *J Oceanogr* 54(4):347–360
- Crosby DS, Breaker LC, Gemmill WH (1993) A proposed definition for vector correlation in geophysics: theory and applications. *J Atmos Ocean Technol* 10:355–367
- Dale WL (1956) Wind and drift current in the South China Sea. *Malay J Trop Geogr* 8:1–31
- Durski SM, Glenn SM, Haidvogel DB (2004) Vertical mixing scheme in the coastal ocean: comparison of the level 2.5 Mellor-Yamada scheme with an enhanced version of the K-Profile parameterization. *J Geophys Res* 109, C01015. doi:10.1029/2002JC001702
- Flather RA (1976) A tidal model of the northwest European continental shelf. *Memories de la Societe Royale des Sciences de Liege* 6(10):141–164
- Gan JP, Li H, Curchitser EN, Haidvogel DB (2006) Modeling South China Sea circulation: response to seasonal forcing regimes. *J Geophys Res* 111:C06034. doi:10.1029/2005JC003298
- Gan JP, Li L, Wang D, Guo X (2009) Interaction of a river plume with coastal upwelling in the northeastern South China Sea. *Cont Shelf Res* 29(4):728–740. doi:10.1016/j.csr.2008.12.002
- Gao J (2013) Evolution of eddies in the northern South China Sea and the characteristics and mechanisms of circulation in the Beibu Gulf. Ph.D. dissertation, Ocean University of China, pp 118 (in Chinese with English abstract)
- Hu JY, Kawamura H, Hong HS, Qi YQ (2000) A review on the currents in the South China Sea: seasonal circulation, South China Sea warm current and Kuroshio intrusion. *J Oceanogr* 56:607–624
- Hu JY, Kawamura H, Tang DL (2003) Tidal front around the Hainan Island, northwest of the South China Sea. *J Geophys Res* 108:3342. doi:10.1029/2003JC001883
- Huang ZD, Hu JY, Sun ZY, Zhu J, Chen ZZ (2008) Distributions of temperature, salinity and density in the eastern Beibu Gulf (Gulf of Tonkin) in spring 2007. The essay collection of the researches on the ocean science in the Gulf of Tonkin-PT II. Ocean Press of China, pp 96–98 (in Chinese with English abstract)
- Li SH (1986) A numerical modeling of the tidal wave in the Beibu Gulf (Gulf of Tonkin). *Trop Oceanogr* 5(3):7–14 (in Chinese with English abstract)
- Li SH (1987) Preliminary study on the eulerian current in the Beibu Gulf. *Trans Oceanol Limnol* 3:8–14 (in Chinese with English abstract)
- Li J, Wang G, Xie S-P, Zhang R, Sun Z (2012) A winter warm pool southwest of Hainan Island due to the orographic wind wake. *J Geophys Oceanogr* 117:C08036. doi:10.10129/2012JC008189
- Liu FS, Yu TC (1980) Preliminary study on the oceanic circulation in Beibu Bay (Gulf of Tonkin). *Trans Oceanol Limnol* 1:9–15 (in Chinese with English abstract)
- Liu AJ, Zhang YT (1997) Numerical prediction and analysis of the tide in Beibu Bay (Gulf of Tonkin). *Chin J Oceanol Limnol* 28(6):640–645 (in Chinese with English abstract)
- Liu QY, Kaneko A, Su JL (2008) Recent progress in studies of the South China Sea circulation. *J Oceanogr* 64:753–762
- Lu XG, Qiao FL, Wang GS, Xia CS, Yuan YL (2008) Upwelling off the west coast of Hainan Island in summer: its detection and mechanisms. *Geophys Res Lett* 35, L02604. doi:10.1029/2007GL032440
- Manh DV, Yanagi T (2000) A study on the residual flow in the Gulf of Tonkin. *J Oceanogr* 56:59–68
- Mellor GL, Yamada T (1982) Development of a turbulence closure model for geophysical fluid problems. *Rev Geophys Space Phys* 20:851–875
- Shaw PT, Chao SY (1994) Surface circulation in the South China Sea. *Deep-Sea Res PT I* 40(11/12):1663–1683
- Shi MC, Chen CS, Xu Q, Lin H, Liu G, Wang H (2002) The role of Qiongzhou Strait in the seasonal variation of the South China Sea circulation. *J Phys Oceanogr* 32:103–121
- Su JL, Yuan YL (2005) Hydrography of China Seas. China Ocean Press, Beijing, pp 367 (in Chinese)
- Sun HL, Huang WM, Zhao JS (2001) Three-dimensional numerical simulation of tide-induced, wind-driven and thermohaline residual currents in the Beibu Bay. *Acta Oceanol Sin* 32(5):1–8 (in Chinese with English abstract)
- Van Maren DS, Hoekstra P (2004) Seasonal variation of hydrodynamics and sediment dynamics in a shallow subtropical estuary: the Ba Lat River, Vietnam. *Estuar Coast Shelf S* 60:529–540
- Wang JF, Wang Y, Sun SW (2008) Tidal currents and residual currents in the southeastern Beibu Gulf (Gulf of Tonkin) in spring. The essay collection of the researches on the ocean science in the Gulf of Tonkin-PT II. Ocean Press of China 53 pp (in Chinese with English abstract)
- Wong LA, Chen JC, Xue H, Dong LX, Su JL, Heinke G (2003) A model study of the circulation in the Pearl River Estuary (PRE) and its adjacent coastal waters: 1. Simulations and comparison with observations. *J Geophys Res* 108(C5):3156. doi:10.1029/2002JC001451
- Wu CR, Shaw PT, Chao SY (1998) Seasonal and interannual variations in the velocity field of the South China Sea. *J Oceanogr* 54(4):361–372
- Wu ZK, Wang LA, Lv XQ, Tian JW, Chen JC (2003) A Numerical model of tides in the Beibu Gulf by adjoint method. *Acta Oceanol Sin* 25(2):128–135
- Wu DX, Wang Y, Lin XP, Yang JY (2008) On the mechanism of the cyclonic circulation in Gulf of Tonkin in the summer. *J Geophys Res* 113, C09029. doi:10.1029/2007JC004208
- Wyrski K (1961) Physical oceanography of the Southeast Asian water. In NAGA report vol. 2, scientific result of marine investigation of the South China Sea and Gulf of Thailand. Scripps Institution of Oceanography, La Jolla, pp 1959–1961, 195pp
- Xia HY, Li SH, Shi MC (1997) Three-D numerical simulation of wind-driven current and density current in the Beibu Gulf. *Acta Oceanol Sin* 20(4):455–472
- Xue H, Chai F (2002) Coupled physical–biological model for the Pearl River estuary: a phosphate limited subtropical ecosystem. In:

- Spaulding ML (ed) Proceedings of the 7th International Conference on Estuarine and Coastal Modeling, ASCE, pp 913–928
- Xue H, Chai F, Pettigrew N, Xu D (2004) Kuroshio intrusion and the circulation in the South China Sea. *J Geophys Res* 109, C02017. doi:10.1029/2002JC001724
- Yang SY, Bao XW, Chen CS, Chen F (2003) Analysis on characteristics and mechanism of current system in west coast of Guangdong Province in the summer. *Acta Oceanol Sin* 25(6):1–8 (in Chinese with English abstract)
- Yu L, Jin X, Weller RA (2008) Multidecade global flux datasets from the Objectively Analyzed Air–Sea Fluxes (OAF flux) Project: latent and sensible heat fluxes, ocean evaporation, and related surface meteorological variables. Woods Hole Oceanographic Institution, OAF flux Project Technical Report. OA-2008-01, 64pp Woods Hole Massachusetts
- Zhang HM, Bates JJ, Reynolds RW (2006) Assessment of composite global sampling: sea surface wind speed. *Geophys Res Lett* 33, L17714. doi:10.1029/2006GL027086
- Zhang GR, Ma T, Pan WR, Lin YH, Wang J (2008) The characteristics of low-frequency flow in the west mouth of Qiongzhou Strait and its response to the seasonal wind field. The essay collection of the researches on the ocean science in the Gulf of Tonkin- PT II, Ocean Press of China, pp 64–76 (in Chinese with English abstract)
- Zu TT (2005) Analysis of the current and its mechanism in the Gulf of Beibu. MS thesis, Ocean University of China, 37pp (in Chinese with English abstract)
- Zu TT, Gan JP, Erofeeva SY (2008) Numerical study of the tide and tidal dynamics in the South China Sea. *Deep-Sea Res I* 55:137–154